

# SPECTRAL PROPERTIES OF LOW FREQUENCY QUASI-PERIODIC OSCILLATIONS IN GRS 1915+105

J. RODRIGUEZ<sup>1,2</sup>, S. CORBEL<sup>3,1</sup>, D.C HANNIKAINEN<sup>4</sup>, T. BELLONI<sup>5</sup>, A. PAIZIS<sup>2</sup>, O. VILHU<sup>4</sup>

*Draft version February 2, 2008*

## ABSTRACT

We report on the timing analysis of *RXTE* observations of the Galactic micro-quasar GRS 1915+105 performed in 2003. Out of a total of six times  $\sim 20$  ks, we focus here only on the three observations during which GRS 1915+105 is found in a steady C-state (referred to as class  $\chi$ ) resulting in a total of  $\sim 50$  ks. During these observations, we detect low frequency quasi-periodic oscillations with high ( $\sim 14\%$ ) rms amplitude in the 2–40 keV energy range. Contrary to what is usually observed in GRS 1915+105, in most of our observations the QPO frequency present no correlation with the *RXTE*/*PCA* count rate, nor with the *RXTE*/*ASM* count rate. We present, for the first time, high resolution (22 spectral channels) 2–40 keV spectral fits of the energy dependence of the QPO amplitude (“QPO spectra”). The QPO spectra are well modeled with a cut-off power law except on one occasion where a single power law gives a satisfactory fit (with no cut-off at least up to  $\sim 40$  keV). The cut-off energy evolves significantly from one observation to the other, from a value of  $\sim 21.8$  keV to  $\sim 30$  keV in the other observations where it is detected. We discuss the possible origin of this behavior and suggest that the compact jet detected in the radio contributes to the hard X-ray ( $\geq 20$  keV) mostly through synchrotron emission, whereas the X-ray emitted below 20 keV would originate through inverse Compton scattering. The dependence of the QPO amplitude on the energy can be understood if the modulation of the X-ray flux is contained in the Comptonized photons and not in the synchrotron ones.

*Subject headings:* accretion, accretion disks — black hole physics — stars: individual (GRS 1915+105)  
 — X-rays: stars

## 1. INTRODUCTION

GRS 1915+105 was discovered by the *WATCH* instrument on-board *GRANAT* in 1992 (Castro-Tirado et al. 1992). It is the first Galactic source observed to have apparent superluminal motion in radio (Mirabel & Rodríguez, 1994), corresponding to the ejection of plasma at a speed of  $\sim 92 - 98\%$  of the speed of light. Its distance is estimated to  $9 \pm 3$  kpc (Chapuis & Corbel 2004), and the mass of the compact object in GRS 1915+105 is estimated to be  $14.0 \pm 4.4 M_{\odot}$  (Harlaftis & Greiner 2004).

Systematic monitoring in the X-rays (mainly with the *Rossi X-ray Timing Explorer*, *RXTE*), revealed a rich pattern of variability on all time scales. GRS 1915+105 is a source of Low and High Frequency QPOs (LFQPO, HFQPO, Morgan, Remillard & Greiner 1997), whose properties (frequency, rms amplitude) are tightly correlated to the spectral parameters (Morgan et al. 1997, Munro et al. 1999, Markwardt et al. 1999, Rodríguez et al. 2002a,b, Vignarca et al. 2002). When analyzing data of black hole binaries, the frequency of LFQPOs have been shown to be best correlated with the slope of the high energy tail of the energy spectra (Vignarca et al. 2002). It should be noted that the LFQPO frequency is usually correlated with the soft X-ray flux, thought to originate from the accretion disk.

Belloni et al. (2000, hereafter B00) analyzing 163 *RXTE*

observations, have shown that, though complex, the behavior of GRS 1915+105 could be understood as spectral transitions between 3 basic states A, B, C. They identified 12 recurrent classes of variability on a timescale of  $\sim 3000$  s. GRS 1915+105 spends most of the time in the so-called  $\chi$  class of variability that corresponds to a steady state in the X-rays, lying in a rather hard part of the color-color diagram (state C or hard state). Based on the X-ray (spectral end temporal) and radio properties of GRS 1915+105, 4 subclasses ( $\chi_1, \chi_2, \chi_3, \chi_4$ ) can be distinguished. Two of them have a high level of radio emission with a flat spectrum, LFQPOs, and a high energy tail (B00, Trudolyubov 2001, Munro et al. 2001, Klein-Wolt et al. 2002).

We monitored GRS 1915+105 with the *INTErnational Gamma-Ray Astrophysics Laboratory* (*INTEGRAL*) during its first AO, for a total of  $6 \times 100$  ks (Hannikainen et al. 2003, 2004), and obtained 120 ks divided in 6 sequences of simultaneous observations with *RXTE*. One of our *RXTE* observations was planned during an *INTEGRAL* target of opportunity on GRS 1915+105, and allowed a wide band simultaneous spectral and temporal coverage to be performed (Fuchs et al. 2003, hereafter F03). The global analysis of the whole campaign is dedicated to a future publication. Here we focus on the timing analysis of the 3 steady C-state *RXTE* observations. The data reduction methods are described in Sec. 2, while the results are presented in Sec. 3 and discussed in Sec. 4

<sup>1</sup>DSM/DAPNIA/Service d’Astrophysique (CNRS FRE 2591), CEA Saclay, 91191 Gif sur Yvette, France

<sup>2</sup>ISDC, Chemin d’Ecogia, 16, 1290 Versoix, Switzerland

<sup>3</sup>Université Paris 7 Denis Diderot, 2 Place Jussieu, 75005 Paris, France

<sup>4</sup>Observatory, PO Box 14, FIN-00014, University of Helsinki, Finland

<sup>5</sup>INAF - Osservatorio Astronomico di Brera via E. Bianchi 46, 23807 Merate (LC), Italy

## 2. OBSERVATIONS AND DATA REDUCTION

The log of the observations analyzed in this paper can be found in Table 1. Each observation covers several satellite orbits. The analysis was first performed on each single revolution, and when no noticeable (spectral or temporal) evolution was found, the different orbits were further averaged to increase the statistics.

We extracted light curves from the *Proportional Counter Array (PCA)* following the standard way described in the Cook Book and ABC of *RXTE*, with the *LHEASOFT V5.3* package. Good time intervals (gti) are defined as follows: satellite elevation over the Earth limb  $> 10^\circ$ , offset pointing  $< 0.02^\circ$ , and PCU 0 and 2 turned on. Light curves were extracted from Binned and Event data. We first accumulated a broad band 2–40 keV (absolute channels 0–94, epoch 5) light curve with the highest time resolution allowed by the (Binned) data format ( $\sim 4$  ms). We then extracted light curves in small energy bins, with the highest spectral resolution allowed by the (Binned) data (16 energy bins from 2 to 14.8 keV), and over 7 additional spectral bins for the Event data (from 15 to  $\sim 40$  keV). Power density spectra (PDS) were produced using *Powspec V1.0*, and corrected for white noise. In the case of the 2–40 keV light curves, PDS were produced on interval length of 64 s between 15.625 mHz and 64 Hz. All intervals were averaged together. The energy dependent PDSs were produced on interval of 160 s length, between 6.25 mHz and 12.8 Hz. Fig. 1 shows, as an example, the PDS's extracted in three energy bands, for Obs.1 We extracted background light curves in all these energy ranges, and used their count rate to obtain the true rms amplitude following Berger and van der Klis (1994). In addition, to check for short term evolution of the QPO frequency, we produced dynamical power spectra with  $\sim 16$  s resolution between absolute channels 0–35 ( $\sim 2 - 14.8$  keV).

## 3. RESULTS

The preliminary spectral analysis (in a multi-wavelength context) of the first observation is presented in F03. The 8 other sequences presented here show similar steady light curves (see Hannikainen et al. 2004, hereafter H04, for details on the *INTEGRAL/RXTE* campaign). The *RXTE/ASM* light curve, showing the dates of our pointed *INTEGRAL/RXTE* observations is represented in Fig. 2. While the long term evolution shows a slow decay, a double flare occurs between Obs. 1 and Obs. 2–7. This X-ray flare is associated with a radio flare (F03), probably indicative of a discrete ejection. We identify the class of variability of our observations as class  $\chi$  of B00. The high level of radio emission detected during each of these observations (F03, H04) allows us to further classify the observations as class  $\chi_1 - \chi_3$  also known as the radio loud hard state (Muno et al. 2001) or type II hard state (Trudolyubov 2001). It should be noted, however, such a long term decay with the source mostly in class  $\chi$  is rather peculiar, and had never been seen previously. A preliminary spectral analysis (F03; H04) shows that the common model of black hole X-ray binaries, i.e. a multicolor disk black body and

a power-law, represents the data well. As mentioned for such classes (Muno et al. 2001), however, the disk temperature returned from the fit is too high (3–4 keV), and the inner radius far too small. Alternative models of broken power-law or broken power-law plus disk component fit the data well and lead to parameters closer to what is seen in other systems (H04). We also successfully fitted the *RXTE/PCA* 3–25 keV spectra with a cut off power-law with a high energy cut-off of about 20–25 keV (Rodriguez et al. 2004, Fig 3). When adding higher energy spectra, such as those extracted with *RXTE/HEXTE*, a large deviation to the spectrum is seen at high energy, indicating the need of an additional spectral component to the model, e.g. an extra power law (Zdziarski et al. 2001; Hannikainen et al. in prep.). This is illustrated in Fig. 3 (left panel) with the particular example of Obs. 1<sup>6</sup>. Furthermore, Rodriguez et al. (2004) have shown that the 20–400 keV combined *RXTE/HEXTE* and *INTEGRAL/IBIS* and *SPI* spectra could be fitted with a power law of photon index  $\sim 3.5$ . Note that similar results were found from the OSSE spectral analysis of Zdziarski et al. (2001).

For all sequences, the 2–40 keV PDS were fitted between  $\sim 15$  mHz and 10 Hz with a sum of 2 or 3 Lorentzians (depending on the energy range), to account for the wide band variability (Belloni, Psaltis & van der Klis 2002). A strong LFQPO is detected in all the PDSs, and is modeled with an additional Lorentzian (harmonics are also detected, especially during intervals with the longest exposures). A first analysis of Obs. 8 showed a rather broad QPO, with parameters poorly constrained. As the dynamical power spectrum showed two distinct features, we separated this observation in sub-intervals and averaged those showing the QPO at the same frequency. This resulted in two distinct sets of data, for which we identified two different QPOs. The LFQPO parameters are reported in Table 2.

At first glance, there is apparently no obvious correlation between the QPO frequency and the PCA 2–60 keV count rate (Tables 1 & 2). To further verify this, we fitted each of the  $\sim 2 - 15$  keV 16 s PDS used to construct our dynamical power spectra with a Lorentzian around the average QPO frequency (Table 2), and could therefore obtain the variations of the QPO frequency with a time resolution of 16 s. No correlation is found between the QPO frequency and the PCA 2 – 15 keV count rate from Obs. 1 through 7, whereas we do find a correlation in Obs. 8.

We further averaged sequences showing the QPO at a similar frequency (Obs. 7, showing the QPO at 1.06 Hz is averaged with Obs. 2 and Obs. 4, whereas Obs. 3, 5 and 6 are averaged together), and produced PDS in the 22 energy bins described in Sec. 2. These energy dependent PDSs were fitted between 6.25 mHz and 10 Hz. The energy dependences of the amplitude of the four distinct features are reported in Fig. 4.

A clear difference in the shape of the energy dependence of the amplitude of the QPO appears in Fig. 4. A clear turn-over in the amplitude vs. energy relation is visible for the  $\sim 2.48$  Hz QPO detected on MJD 52731, and another one is visible for the  $\sim 1.09$  Hz QPO from the observa-

<sup>6</sup>Note that the details of the *RXTE* and *INTEGRAL* spectral analysis will be given in a forthcoming paper, dedicated to the spectral analysis of the whole campaign. However, the *RXTE* (PCA, and *HEXTE*) spectra have been extracted in the same way as in, e.g., Rodriguez et al. 2003.

tion of MJDs 52738-52739, although it is not as clear as for the first QPO. For the three other features we do not see any clear turn-over (Fig. 4), although a flattening is obvious at energies above 10 keV. This may suggest that the turn-over energy evolves from one observation to the other, and is above the upper energy limit of our QPO "spectra". To further test this hypothesis, we fitted the QPO spectra in *XSPEC V11.3.0*. For all QPOs but the 1.04 Hz one, the spectra are well fitted by a cut-off power-law (cutoffpl in *XSPEC*). The fit parameters are reported in Table 3, while the right panel of Fig. 3 shows the QPO spectrum of Obs. 1 with the best fit model superimposed. It should be added here that a single power law gives a rather good representation of the 1.878 Hz QPO detected in Obs. 8, with a reduced chi square of 1.89 (20 dof). A cut-off power law model improve the fit (Table 3), although the cut-off energy is poorly constrained (4.7- $\sigma$  significance on this parameter). It is interesting to note that the break energy seems anti-correlated with the QPO frequency, i.e. the lowest break energy is observed for the highest QPO frequency (Table 3). Caution has to be expressed, however, since the statistical uncertainties on the break energies does not allow us to draw firm conclusion.

#### 4. DISCUSSION

The presence of LFQPO in GRS 1915+105 during class  $\chi$  (as well as during other classes) is a known fact (e.g. Munro et al. 1999, Rodriguez et al. 2002a,b). It is also known that QPO parameters depend on spectral parameters in black hole binaries (BHB) in general. Here we present observations taken during the same state, with few differences between the spectral parameters returned from the spectral fits. The parameters of the QPO change dramatically from one observation to another. Except in Obs. 8, the frequency of the QPO does not seem to correlate to the *PCA* 2–15 keV flux or the *ASM* 1.2–12 keV flux either (although the highest frequency is observed when the *ASM* flux is the highest, Fig. 2, and Table 2), contrary to what is usually claimed/observed. This could indicate some definite peculiarities in Obs. 1-7 that are taken just before and after the X-ray/radio flare (Fig. 2, F03). On the other hand, Obs. 8 occurs later, after GRS 1915+105 apparently went off the linear decay phase, after the *ASM* light curve showed some variability again.

The most striking behavior appears when studying the energy dependence of the QPO amplitude. It is expected and a known fact that it presents a turn-over at some point (e.g. Tomsick & Kaaret 2001, Rodriguez et al. 2002a). We report here, for the first time, a clear evolution of the turn-over energy between states that are spectrally similar, and have similar *PCA* fluxes. This "cut-off" energy has an origin that is unclear. It could represent, for example, some specific temperature at which the QPO is produced, either through oscillations of a shocked boundary layer between the accretion disk, and a hot inner flow (e.g. Chakrabarti & Titarchuk 1995), or by a hot spot orbiting at some specific radius in the disk (e.g. Rodriguez et al. 2002a; Tagger et al. 2004). In these two cases, however, we would expect the frequency of the QPO to scale with the inner radius of the accretion disk, and thus the soft X-ray flux (Molteni, Sponholz & Chakrabarti 1996; Tagger & Pellat 1999), unless the soft X-rays are not uniquely produced by the accretion disk, but by another physical medium, as

e.g. a compact jet (see Markoff & Nowak 2004). The variations of the soft X-rays flux could be due to variations of the compact jet flux (with a steady thermal flux from the accretion disk), as we discuss below.

The spectral approach presented in H04, and Rodriguez et al. (2004), the systematic analysis of type II states (Trudolyubov 2001), and the detection of a hard tail up to (at least) 600 keV with OSSE (Zdziarski et al. 2001) raise the challenging question of the origin of the third spectral component needed to fit the high energy spectra well. Models of jet emission (e.g. Markoff et al. 2003, Markoff & Nowak 2004) propose a jet model in which the X-ray spectrum of an XRB would represent the sum of thermal emission from the accretion disk, direct synchrotron from the jet, inverse Comptonization (either through synchrotron self-Compton from the jet, or Comptonization on the basis of the jet, the "corona"), reflection of these radiations on the accretion disk. It should be noted This proposition has found an echo with the radio flux/X-ray flux correlation found in several BHBs when in the low hard state (when the compact jet is present, e.g. Corbel et al. 2003, Gallo et al. 2003), but also in the case of radio loud AGN (e.g. Merloni, Heinz & di Matteo, 2003; Falcke, Körding & Markoff, 2004). Our RXTE observation of MJD 52731 occurred at a time when the radio flux was high and indicative of the presence of the compact jet (F03). The level of radio emission as measured by the Ryle telescope at 15 GHz is about 130-150 mJy during this observation, with a spectrum extending up to the near infra-red range (F03). Unfortunately we do not have such a nice coverage for the following observations, but the observation of MJDs 52738-52739 indicates a level of 15 GHz emission higher ( $\sim 250$  mJy, F03), that is dropping rapidly. We remark that this observation occurred just after a radio flare indicative of a discrete ejection. It is thus very likely that the radio emission this day partly originates from the discrete ejection (with a different spectrum). During the last observation, the radio flux is very low compared to the two previous dates, with a level dropping from 107 mJy on MJD 52767 to 44 mJy on MJD 52769 (H04). Both our spectral analysis (H04, Rodriguez et al. 2004) and the properties of the QPOs (present work) can be understood easily, if the X-ray emission in GRS 1915+105 during radio loud/type II/class  $\chi_1 - \chi_3$  observations originate (as proposed by Markoff & Nowak 2004) from two different physical processes (beside the thermal emission of the accretion disk): Comptonization and synchrotron radiation. The high energy spectrum of a source with a compact jet represents thus the sum of these different emission processes. As a result the spectrum will therefore strongly depend on the relative contribution of each of these emission processes. The break in the energy spectrum could be representative of the energy at which the relative contributions of these components cross each other. Above the break the contribution of the synchrotron radiation would be the dominant process to the spectrum. Then the higher the relative contribution of the synchrotron component (to the overall spectrum) the lower the break energy is. In this case, to understand the energy dependence of the QPO amplitude, one has to assume that the QPO is contained in the Comptonized flux, and not in the synchrotron flux. Then the position of the cut-off in the energy dependence



of the QPO amplitude would be linked to the synchrotron flux emitted by the jet. We find this interpretation at least qualitatively in good agreement with several observational facts:

- the compact jet model has successfully been used in the fitting of different BHBs (e.g. Markoff et al. 2001).
- type II states show a 2–30 keV level of variability lower than that of type I (radio quiet) states (Trudolyubov 2001).
- a compact jet is detected during the observation showing the clear and well constrained cut-off in the energy dependence of the QPO amplitude (Obs. 1, Fig. 4)
- a high level of radio emission is detected during the observation taken on MJDs 52738–52739, a turn-over in the energy dependence of the  $\sim 1.09$  Hz QPO is detected (Fig. 4, Table 3, although it is absent in the spectrum of the  $\sim 1.04$  Hz QPO), while for the last observation (MJD 52768) the radio flux is much lower, a single power law can fit the first QPO spectrum, and the turn over is poorly constrained (Fig. 4, Table 3).

We should add that the Optical/UV/X-ray variability (and presence of LFQPO in those bands) seen in XTE J1118+480 (Hynes et al. 2003), a Black Hole X-ray transient in which the compact jet model has been shown to fit the broad band spectra well (Markoff et al. 2001), is also compatible with our interpretation. Hynes et al. (2003) pointed out that the variability could not originate from the disk itself, but involved another non-thermal source of photons.

The lack of complete simultaneity, between the radio and X-ray observations, prevents us from drawing any firmer conclusions. In addition, a cut-off in the spectrum of the compact jet is expected in the near infra-red domain. Knowing its exact position would allow us to estimate the flux expected from the jet in the hard X-rays accurately, and thus test our hypothesis. We hope to obtain such simultaneous coverages in the near future, with *INTEGRAL*, *RXTE* for the high energies, but also the Ryle telescope and the VLA, in the radio domain, and *Spitzer*, and ground based telescopes in the infra red domain.

The authors would like to thank G. Henri for useful discussions and G. Pooley for kindly providing the Ryle data to our group. J.R. acknowledges financial support from the French Space Agency (CNES). DCH acknowledges the Finnish Academy.

#### REFERENCES

- Belloni T., Klein-Wolt M., Méndez M., et al. 2000, A&A, 355, 271, **B00**.  
 Belloni T., Psaltis D., van der Klis M. 2002, ApJ, 572, 392.  
 Berger M. & van der Klis M., 1994, A&A, 292, 175.  
 Castro-Tirado A.J., Brandt S., Lund N. 1992, IAUC 5590.  
 Chappuis C. & Corbel S. 2004, A&A, 414, 659.  
 Chakrabarti S.K., Titarchuk L. G., 1995, ApJ, 455, 623.  
 Corbel S., Nowak M., Fender R.P., Tzioumis A. K., Markoff S. 2003, A&A, 400, 1007.  
 Falcke H., Körding E., Markoff S., 2004, A&A, in press, astro-ph/0305335  
 Fuchs Y., Rodriguez J., Mirabel I.F., et al. 2003, A&A, 409, L35, **F03**.  
 Gallo E., Fender R.P., Pooley G.G. 2003, MNRAS, 344, 60.  
 Hannikainen D.C., Vilhu O., Rodriguez J., et al. 2003, A&A 411, L415.  
 Hannikainen D.C., Vilhu O., Rodriguez J., et al. 2004, Proceedings of the 5<sup>th</sup> INTEGRAL workshop, **H04**.  
 Harlaftis E. T. & Greiner J. 2004, A&A, 414, L13.  
 Hynes R. I., Haswell C. A., Cui W., et al. 2003, MNRAS, 345, 292  
 Klein-Wolt M., Fender R.P. Pooley G.G. et al. 2001, MNRAS, 331, 745.  
 Markoff S., Falcke H., Fender R.P. 2001, A&A, 372, L25.  
 Markoff S., Nowak M., Corbel S., Fender R., Falcke H. 2003, A&A, 397, 645.  
 Markoff S. & Nowak M. 2004, ApJ in press, astro-ph 0403468.  
 Markwardt C.B., Swank J.H., Taam R.E., 1999, ApJ, 513, 37.  
 Merloni A., Heinz S., di Matteo T., 2003, MNRAS, 345, 1057  
 Mirabel I.F., Rodriguez L.F. 1994, Nature, 371, 46.  
 Molteni D., Sponholz H., Chakrabarti S.K., 1996, ApJ, 457, 805.  
 Morgan E.H., Remillard R.A., Greiner J. 1997, ApJ, 482, 993.  
 Munro M. P., Morgan E. H., and Remillard R. A. 1999, ApJ, 527, 321.  
 Munro M.P., Remillard, R.A., Morgan, E.H., et al. 2001, ApJ, 556, 515.  
 Rodriguez J., Durouchoux P., Mirabel F., Ueda Y., Tagger M., Yamaoka K. 2002a, A&A, 386, 271.  
 Rodriguez J., Varnière P., Tagger M., Durouchoux P. 2002b, A&A 387, 487.  
 Rodriguez J., Corbel S., Tomsick J.A. 2003, ApJ 595, 1032.  
 Rodriguez J., Fuchs Y., Hannikainen et al. 2004, Proceedings of the 5<sup>th</sup> INTEGRAL workshop, astro-ph 0403030.  
 Tagger M. & Pellat R., 1999, A&A, 349, 1003.  
 Tagger M. Varnière P., Rodriguez J., Pellat R., 2004, ApJ, in press, astro-ph 0401539.  
 Tomsick J.A., Kaaret P., 2001, ApJ, 548, 401.  
 Trudolyubov S. 2001, ApJ, 558, 276  
 Vignarca F., Migliari S., Belloni T., Psaltis D., van der Klis M. 2003, A&A, 397, 729.  
 Zdziarski A.A., Grove E.J., Poutanen J., Rao A.R., Vadawale S.V. 2001, ApJ, 554, L45.

TABLE 1

LOG OF THE RXTE OBSERVATIONS USED IN THE PRESENT ANALYSIS. THE FIRST OF THESE OBSERVATIONS WAS PERFORMED SIMULTANEOUSLY WITH THE MULTI-WAVELENGTH CAMPAIGN DISCUSSED IN FUCHS ET AL. (2003). OBSERVATIONS ARE TIME ORDERED. \* CTS/S IN THE TOP LAYER OF PCU #2, BOTH ANODES.

Observation #	Obs. Date (MJD)	Obs. Id. (P80127-)	Good Time (s)	Number of PCU	Net Count Rate /PCU*
1	52731	01-03-00	9,300 s	4	1737.5 cts/s
2	52738	02-01-00	5,400 s	3	1700.8 cts/s
3	52739	02-02-02	1,800 s	3	1675.8 cts/s
4		02-02-01	1,800 s	4	1666.9 cts/s
5		02-02-00	2,060 s	3	1660.4 cts/s
6		02-03-00	11,100 s	3-4	1674.7 cts/s
7		02-01-01	3,200 s	3	1677.0 cts/s
8	52768	03-01-00	14,000	3-4	1460.2 cts/s

TABLE 2

PARAMETERS OF THE LFQPO DETECTED IN EACH OF THE 8 SEQUENCES. \*  $Q = \frac{\text{Centroid frequency}}{FWHM}$

Obs. sequence	QPO frequency (Hz)	Q*	rms amplitude %
1	$2.498 \pm 0.005$	5.0	$12.6 \pm 0.3$
2	$1.040 \pm 0.004$	3.8	$13.5 \pm 0.6$
3	$1.081 \pm 0.004$	7.2	$13.2^{+1.0}_{-0.9}$
4	$1.039 \pm 0.004$	7.2	$12.7^{+1.2}_{-1.3}$
5	$1.097 \pm 0.005$	10.0	$11.5 \pm 1.0$
6	$1.096 \pm 0.002$	6.4	$13.4 \pm 0.4$
7	$1.060 \pm 0.003$	6.4	$13.0 \pm 0.9$
8_QPO1	$1.878^{+0.005}_{-0.003}$	6.8	$12.9 \pm 0.5$
8_QPO2	$2.332 \pm 0.005$	5.3	$14.9 \pm 0.5$

TABLE 3

PARAMETERS OF THE FITS TO THE ENERGY DEPENDENCE OF THE QPO AMPLITUDE, ALSO REFER TO AS QPO SPECTRA IN THE TEXT. THE ERRORS ARE GIVEN AT THE ONE- $\sigma$  LEVEL. \* NO CUT-OFF IS DETECTED IN THIS OBSERVATION AT LEAST UP TO  $\sim 40$  KEV.

QPO freq. (Hz)	Power-law slope ( $\Gamma$ )	Cut-off energy (keV)	reduced $\chi^2$ (dof)
2.498	$-0.77 \pm 0.04$	$21.9^{+2.7}_{-2.2}$	1.0 (19)
1.04	$-0.26 \pm 0.02$	No cut-off*	0.92 (21)
1.09	$-0.59 \pm 0.05$	$29.5^{+5.2}_{-3.9}$	0.37 (20)
1.878	$-0.70 \pm 0.07$	$25.6^{+6.5}_{-4.4}$	0.5 (19)
2.332	$-0.71 \pm 0.05$	$26.7^{+4.4}_{-3.3}$	0.28 (20)

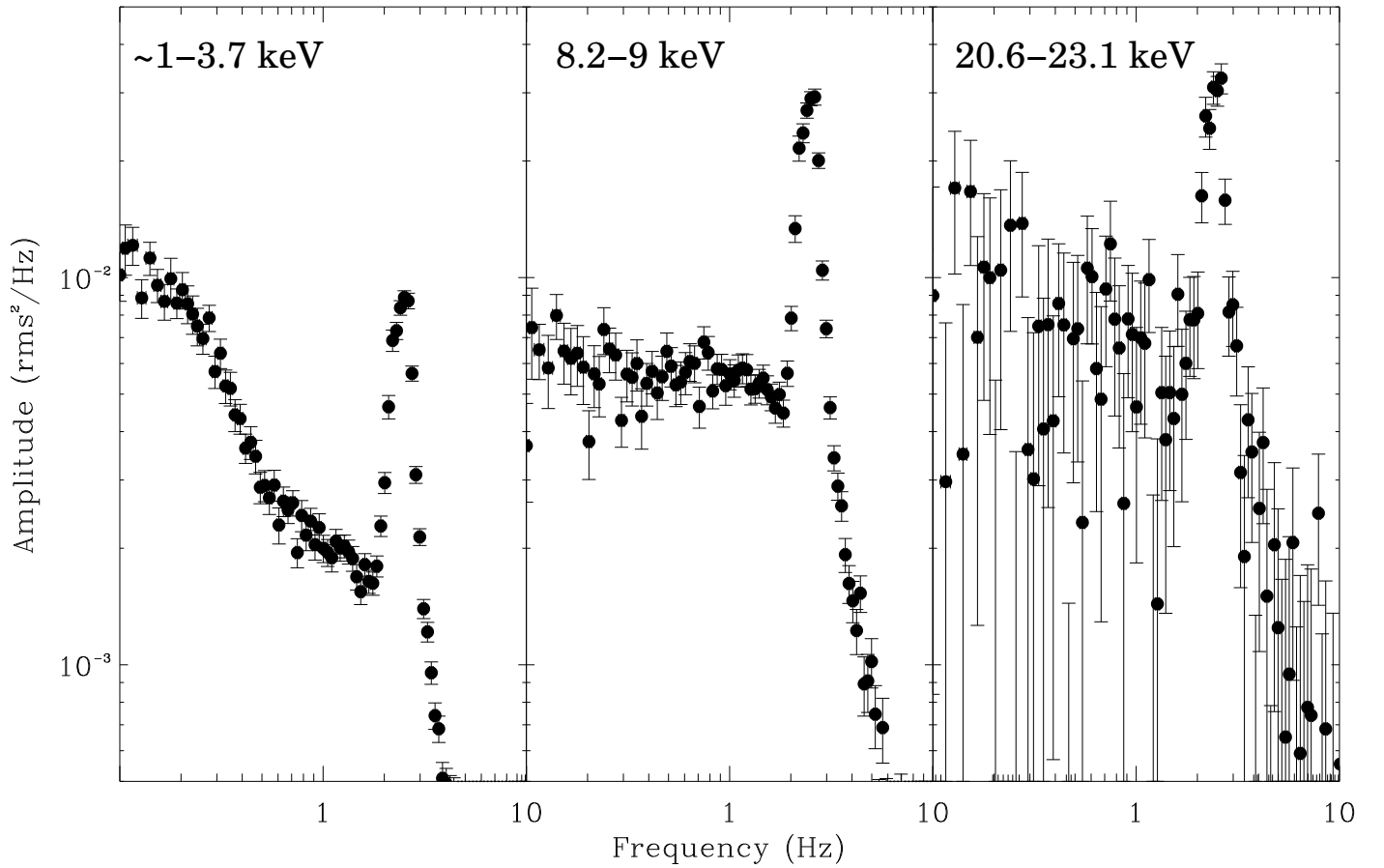


FIG. 1.— Example of PDS's extracted in three energy bands (1–3.7 keV, 8.2–9 keV, and 20.6–23.1 keV), as described in the text. These PDS's are from Obs. 1. The 2.498 Hz LFQPO is obvious in each panel. The same vertical scale is used for each PDS and allows for a direct comparison of the source behavior in those energy bands.

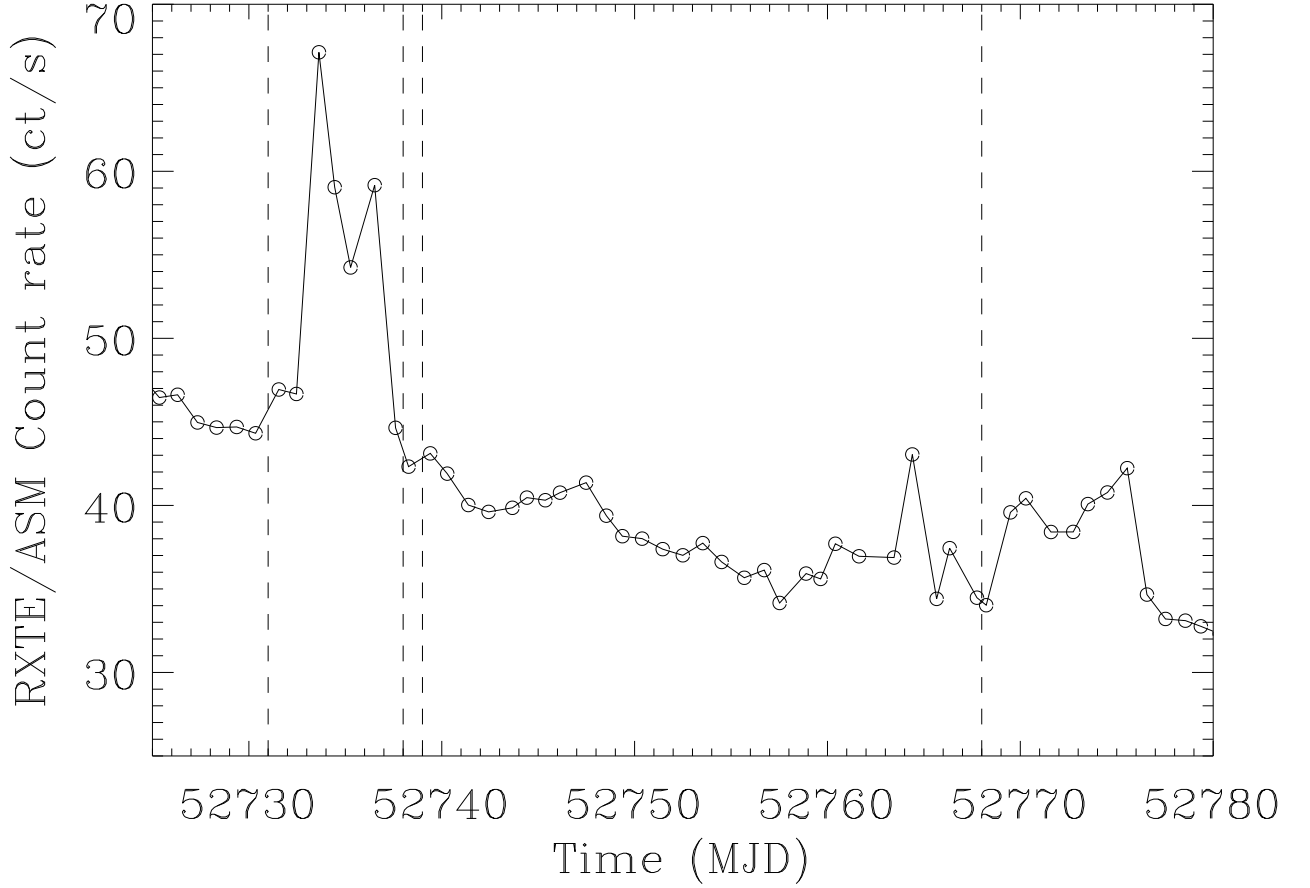


FIG. 2.— RXTE/All Sky Monitor 1.2–12 keV light curve of GRS 1915+105. The vertical dashed lines show the days our observations took place. The 1.2–12 keV  $\sim 1$  Crab flare is obvious here. A radio flare is detected at the same time, with its maximum occurring 2 days later (F03).

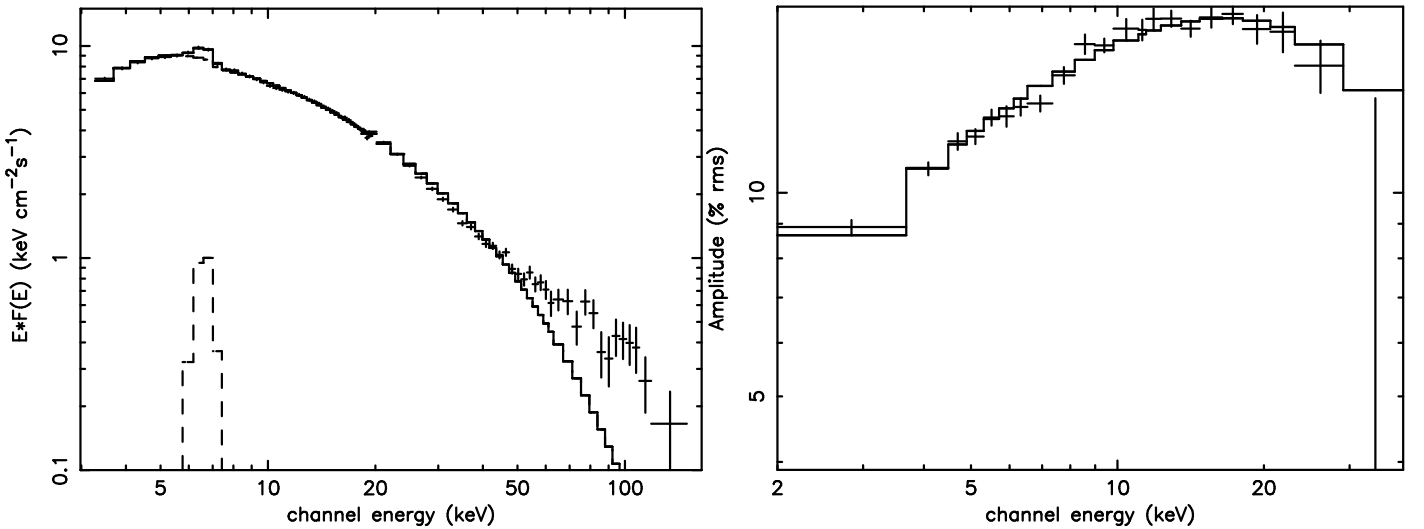


FIG. 3.— *Left panel:* PCA+HEXTE 3–150 keV  $\nu - f_\nu$  spectra from Obs. 1. A model consisting of an absorbed power law with a high energy cut-off of about 25 keV (plus a Gaussian at 6.4 keV) is superimposed. The deviation to this model at high energy is obvious here. This likely reflects the need of an additional component to account for the high energy emission from GRS 1915+105. *Right panel:* Energy dependence of the QPO amplitude observed during the same observation. The best fit model a power law with a high energy cut-off of  $\sim 22$  keV is superimposed.

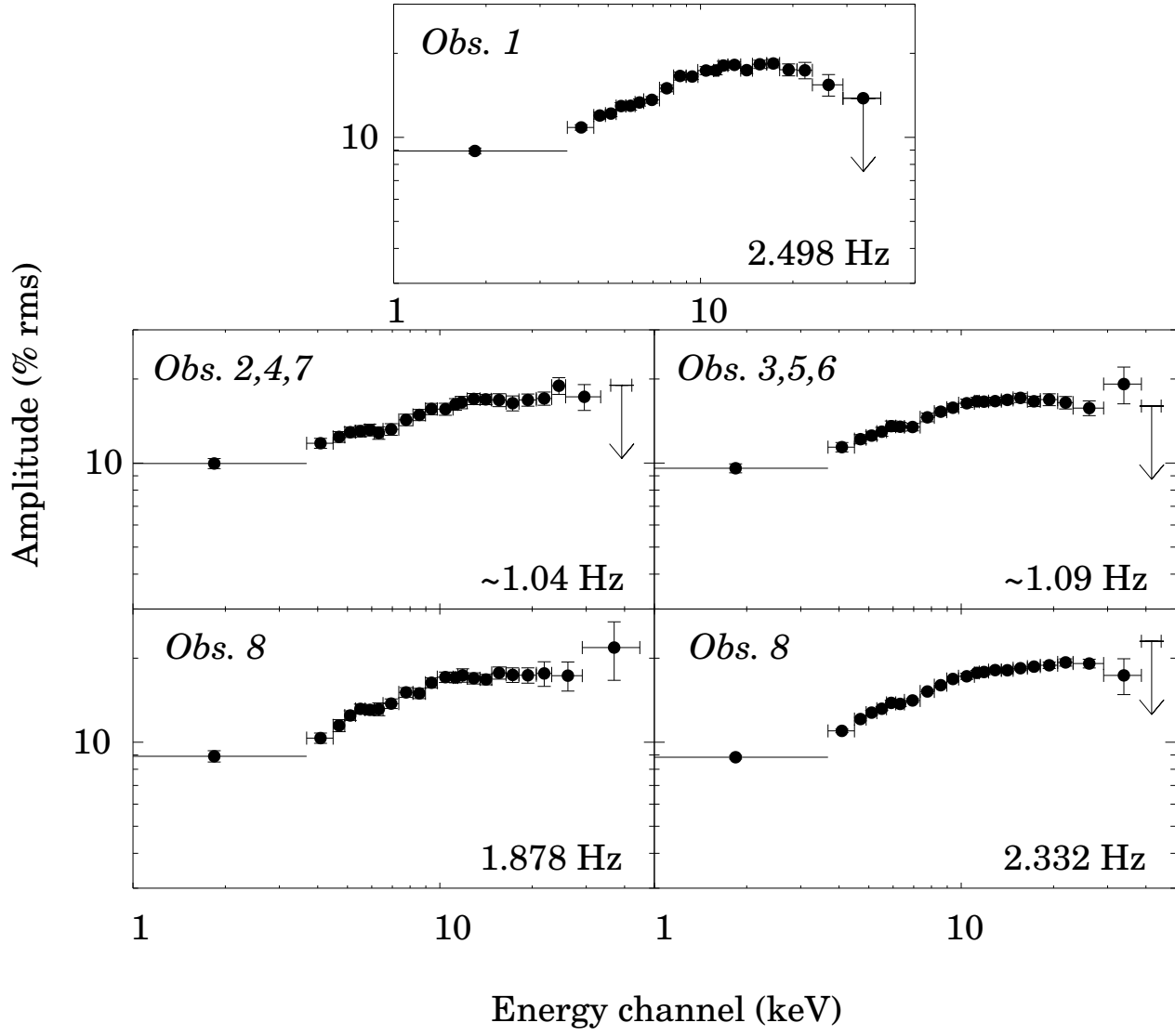


FIG. 4.— Energy dependence of the LFQPO amplitude. The frequency (or mean frequency) of the feature and the observation numbers are written in each panel.